Uetake *Earth, Planets and Space* (2017) 69:71
DOI 10.1186/s40623-017-0655-x

Earth, Planets and Space

LETTER

Open Access

Effects of subsurface structures of source regions on long-period ground motions observed in the Tokyo Bay area, Japan

Tomiichi Uetake*

Abstract

We compared the long-period ground motion observed in the Tokyo Bay area during two shallow M6.7 earthquakes that occurred in northern Nagano Prefecture, Japan, on March 12, 2011, and November 22, 2014. The magnitudes, focal depths, and source mechanisms of these events were almost identical, but their seismograms were quite different. Significant long-period later arrivals with a predominant period of 5 s were recognized in the velocity traces of the 2011 event, but there were no such remarkable later arrivals in the 2014 event traces. The ground motions at stations located outside the basin area were studied as incident waves to the Kanto Basin. A large wave packet with a predominant period of 5 s was recognized in the velocity traces of the 2011 event, but there was no significant wave packet in the 2014 event traces. Based on particle motion, this wave packet was hypothesized to be a Rayleigh wave. The source regions of the two events have quite different subsurface structures. The different characteristics in long-period ground motion in the Tokyo Bay area during the two events were due to different Rayleigh wave excitations in the source regions.

Keywords: Long-period ground motion, Rayleigh wave, Velocity structure, Source region, Kanto Basin

Introduction

A shallow M6.7 earthquake occurred in northern Nagano Prefecture, Japan, on November 22, 2014. This event was the first M7 class event to occur in this area after a shallow M6.7 earthquake occurred at the Niigata–Nagano prefectural border on March 12, 2011. The epicenters of these events are shown in Fig. 1. These two events had the same magnitude, according to the Japan Meteorological Agency (JMA) earthquake catalog (Japan Meteorological Agency 2016) and similar source mechanisms, according to the F-net moment tensor solution (Fukuyama et al. 1998; Okada et al. 2004). Both epicenters were located northwest of Tokyo Bay, and the distances from Tokyo Bay were comparable. Usually, ground motion characteristics are estimated based on source parameters, path distance, and site conditions (e.g., Kanno et al. 2006; Yokota et al. 2011; Yuzawa and Nagumo 2012). Considering this, although the ground motions observed in the Tokyo Bay area during these two events should have shown similar characteristics, their seismograms showed some differences. Such differences are usually considered to be due to deviations in ground motion in an empirical evaluation. In this paper, we describe the waveforms around the Tokyo Bay area during the two events and discuss the causes of their different characteristics.

Events and observation stations used in this study

We studied observation data from two shallow earthquakes that occurred in northern Nagano Prefecture, Japan. One event occurred at the Niigata–Nagano prefectural border in 2011; the other occurred in the northern part of Nagano Prefecture in 2014. The source parameters of these two events are shown in Table 1. According to the JMA, the magnitudes of both the events are the same, but the focal depth of the 2011 event is deeper than the focal depth of the 2014 event (Japan Meteorological Agency 2016). According to F-net (Fukuyama et al. 1998; Okada et al. 2004), the moment magnitude of the 2011

*Correspondence: uetake.tomiichi@tepco.co.jp
TEPCO Research Institute, Tokyo Electric Power Company Holdings, Inc., 4-1 Egasaki-cho, Tsurumi-ku, Yokohama, Kanagawa 230-8510, Japan

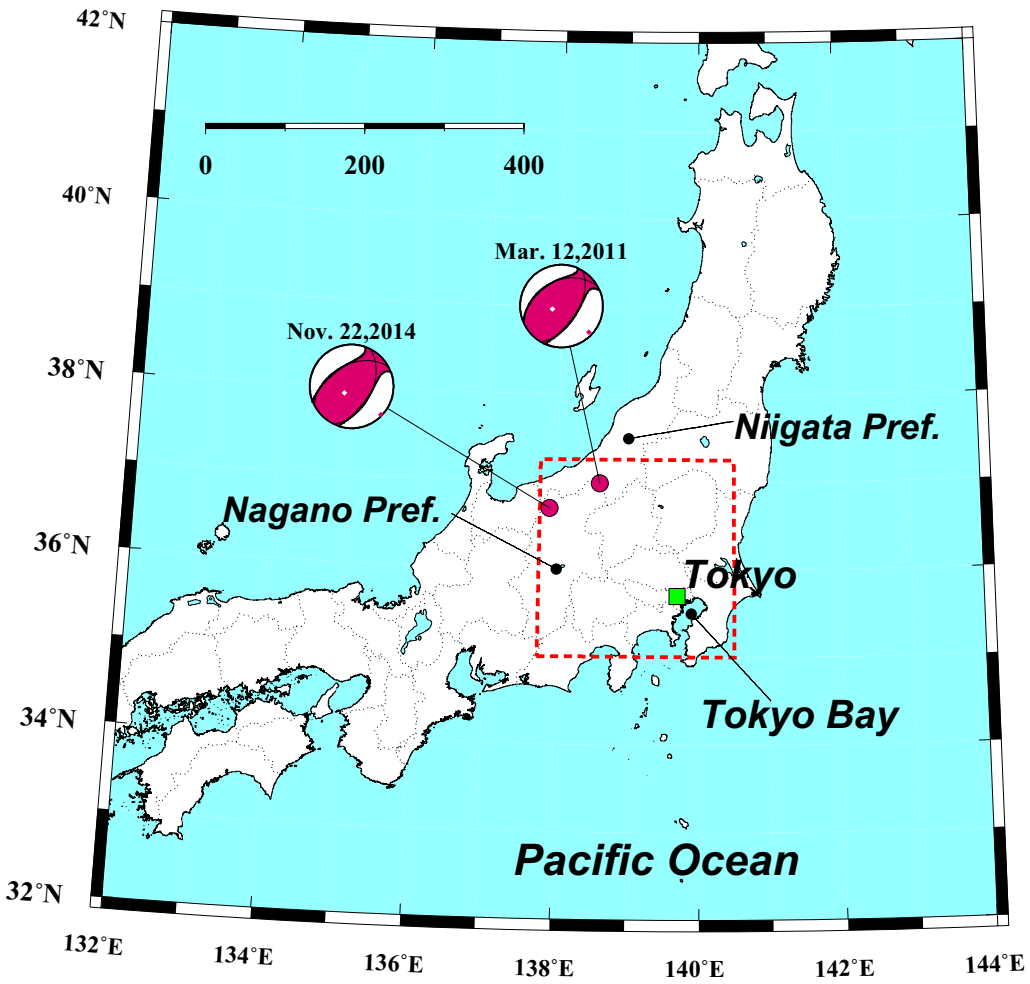

Fig. 1 Epicenters of the events used in this study. The area in the *red square* is enlarged in Fig. 2. *Dashed lines* show the prefectural borders in Japan. The event source mechanisms are the moment tensor solutions from F-net (Okada et al. 2004)

Table 1 Event source parameters

Date	Time (JST)	Epicenter		JMA		F-net	
		Latitude	Longitude	*M*	Depth (km)	Mw	Depth (km)
March 12, 2011	03:59	36.986N	138.598E	6.7	8.4	6.2	5
November 22, 2014	22:08	36.693N	137.891E	6.7	4.6	6.3	5

event is slightly smaller than that of the 2014 event, but the focal depths are the same; furthermore, both source mechanisms are almost identical. The epicenters and source mechanisms of these events are shown in Figs. 1 and 2. The locations of the two events are different, but the source parameters are almost identical. The observation stations used in this study are shown in Fig. 2. The distance and back azimuth of the 2011 event from the SNG station on the west shore of Tokyo Bay are about 184 km and N325°E, respectively. Those of the 2014 event are about 206 km and N305°E, respectively. The differences in distance and back azimuth from the Tokyo Bay area are about 20 km and 20°, respectively.

In this study, we consider data from two networks. One is the broadband velocity seismometer network on the shore of Tokyo Bay, operated by Tokyo Electric Power Company Holdings (TEPCO). The green squares in Fig. 2 indicate the TEPCO stations. Servo velocity

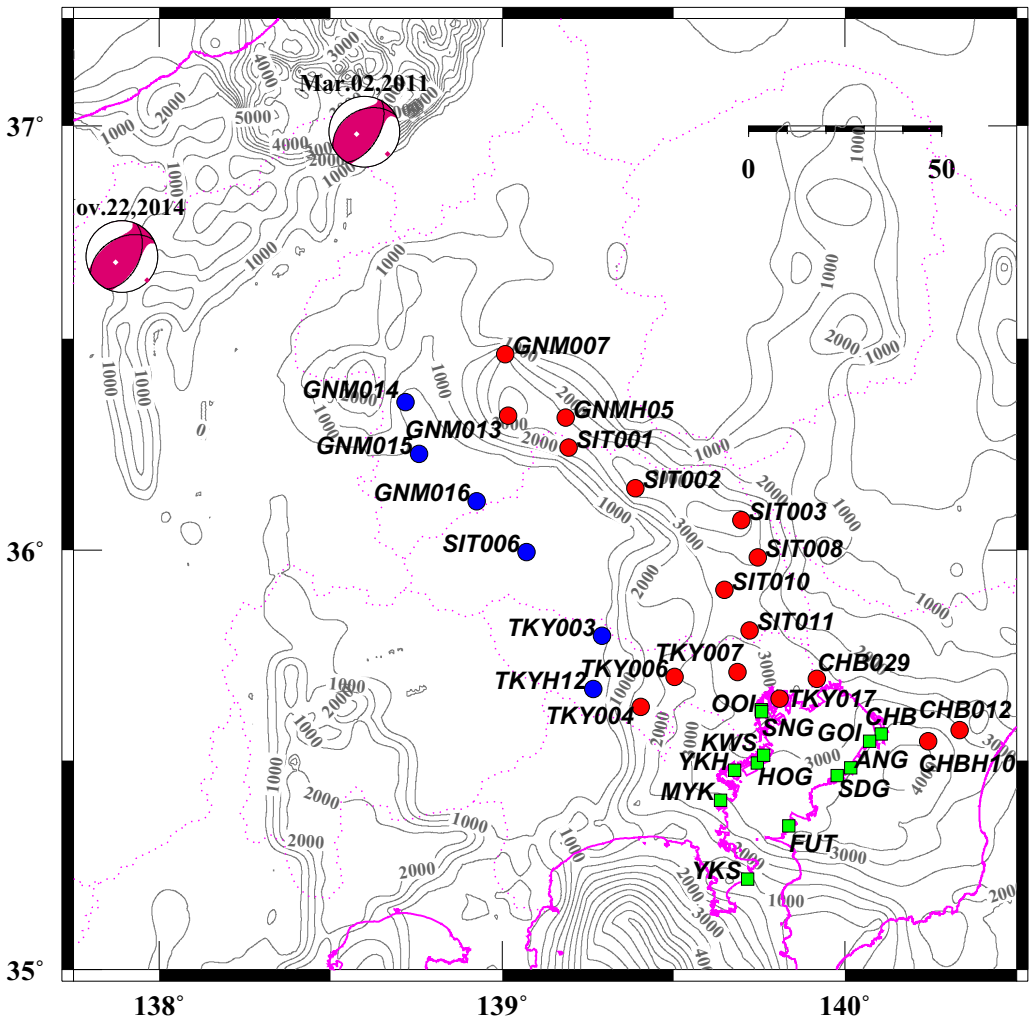

Fig. 2 Locations of the strong motion observation stations used in this study. *Green squares* indicate the Tokyo Electric Power Company Holdings stations. *Circles* indicate K-NET and KiK-net stations (Okada et al. 2004). *Red circles* show the stations located in the basin area, and *blue circles* show the stations located outside the basin. Characters next to *each mark* indicate the station code. *Dashed purple lines* show the prefectural borders in Japan. *Gray contour lines* indicate the depth of seismic bedrock from the "Japan Integrated Velocity Model version 1" (Koketsu et al. 2012). Event source mechanisms are the moment tensor solutions from F-net (Okada et al. 2004)

seismometers (Tokyo Sokushin VSE-355G3) are installed in TEPCO's network. The full scale of the sensor is 2 m/s, and the sensor response is flat in the frequency range between 0.008 and 70 Hz. The data are recorded with 100-Hz sampling and 24-bit resolution. The other data are from the strong motion seismograph networks (K-NET and KiK-net) operated by the National Research Institute for Earth Science and Disaster Resilience, Japan (NIED) (Okada et al. 2004). The red and blue circles in Fig. 2 show the NIED stations used in this study. Feedback-type high-resolution accelerometers are installed at the K-NET and KiK-net stations. Because we primarily discuss the characteristics of velocity waveforms, the acceleration data were integrated into the velocity traces in the frequency domain.

The gray contours in Fig. 2 indicate the depth of seismic bedrock from the "Japan Integrated Velocity Structure Model Version 1" (Koketsu et al. 2012). The upper boundary of the seismic bedrock around Tokyo Bay is very deep, about 3000–4000 m. The contour also suggests that the velocity structures in the source regions of the two events are different. The depth of seismic bedrock in the source region of the 2011 event is deeper than the source region of the 2014 event.

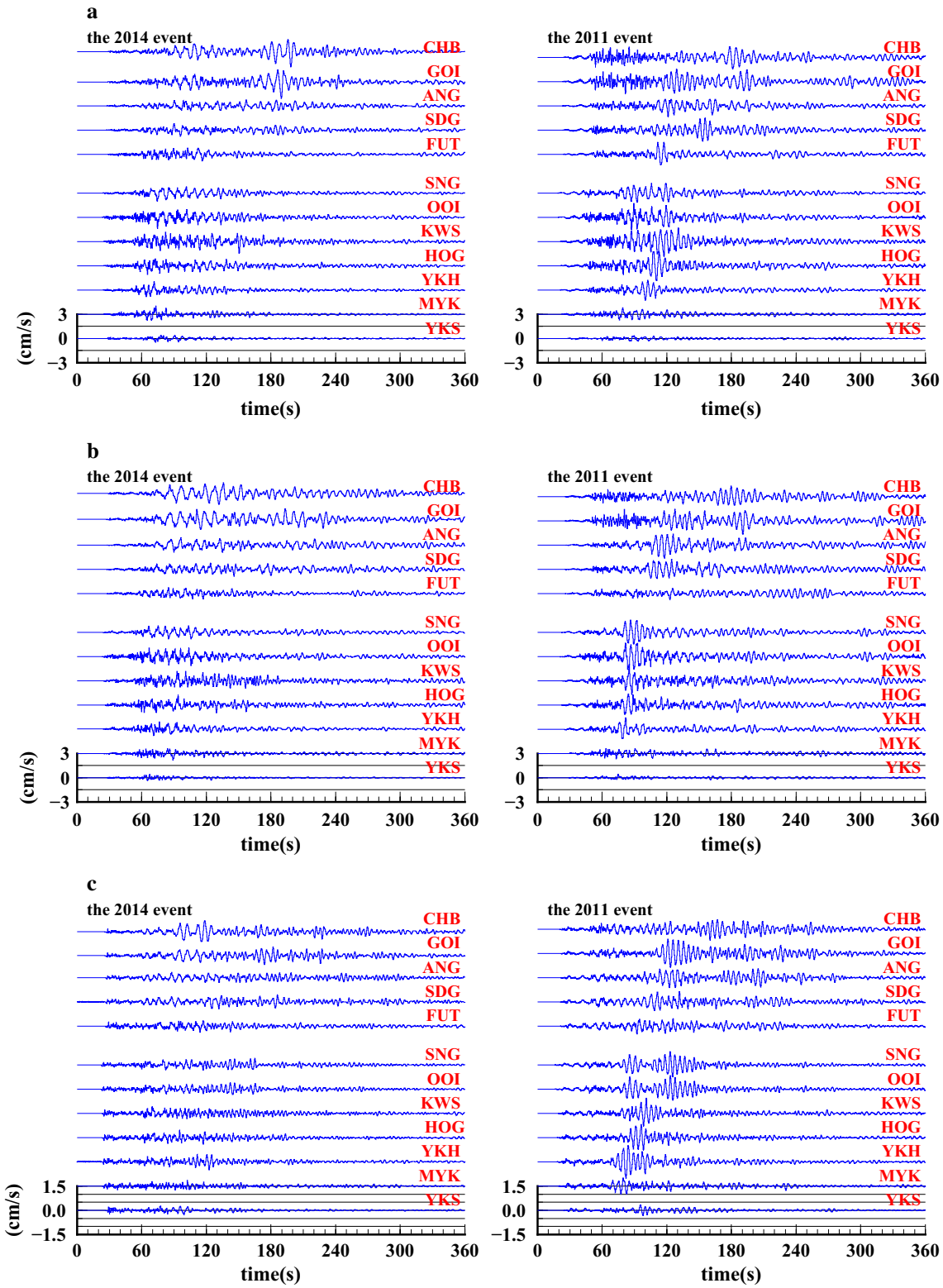

Fig. 3 Velocity seismograms observed at TEPCO stations in the Tokyo Bay area, **a** NS component, **b** EW component, and **c** UD component. The *left side* shows the records for the 2014 event, and the *right side* shows the records for the 2011 event. *Red characters associated with each trace* indicate the station code. The location of each station is shown in Fig. 2

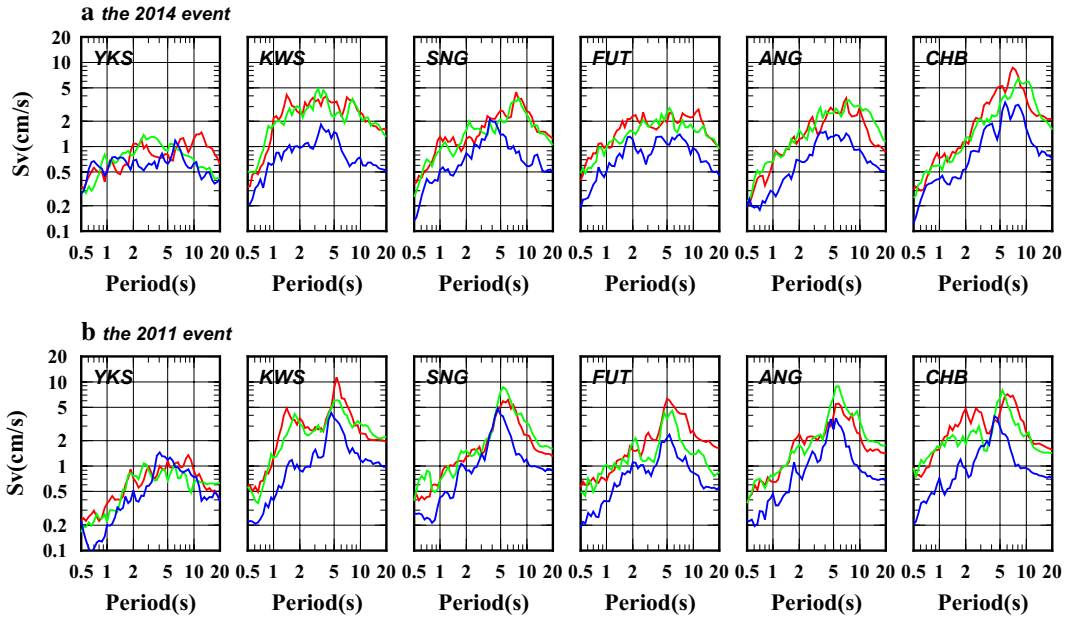

Fig. 4 Velocity response spectra with 5% damping for the Tokyo Bay area stations. **b** Show the spectra from the 2011 event. **a** Show those from the 2014 event. *Red*, *green*, and *blue lines* indicate the spectra for the NS, EW, and UD components, respectively. *Characters in each frame* indicate the station code. The location of each station is shown in Fig. 2

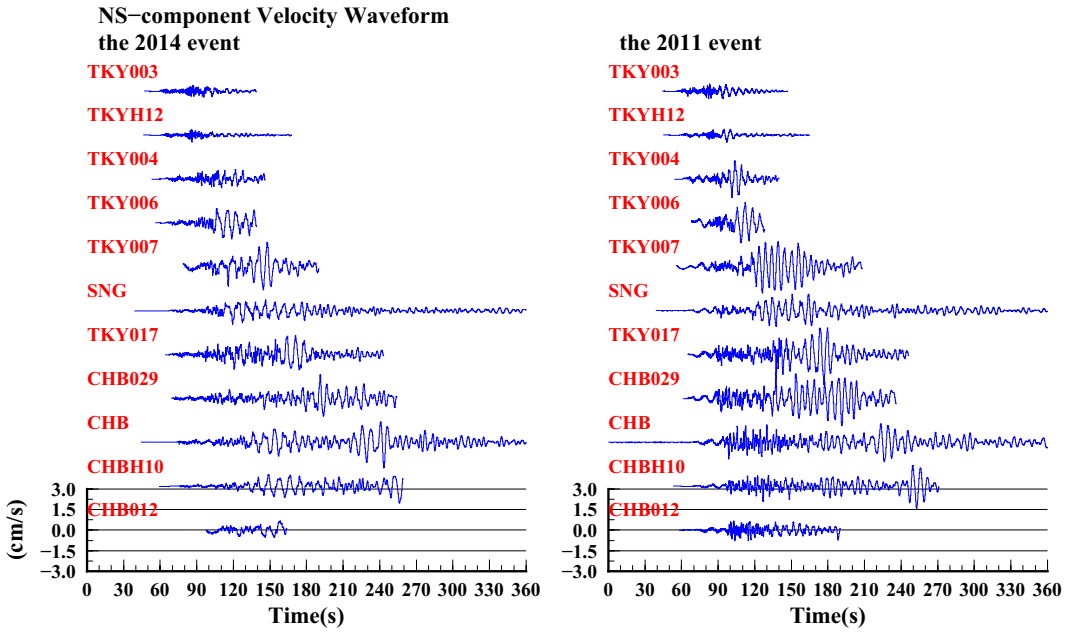

Fig. 5 Comparison of NS component velocity seismograms between the 2014 and 2011 events at stations on a west–east observation line in northern Tokyo Bay. *Characters associated with each trace* indicate the station code. The location of each station is shown in Fig. 2

Velocity seismograms observed around the Tokyo Bay area

The velocity seismograms of both events observed at the TEPCO stations are shown in Fig. 3. There are some differences between the velocity waveforms of the 2011 and 2014 events. Remarkable wave packets are recognized in the waveforms of the 2011 event for all components; these remarkable later arrivals have a predominant period of about 5 s. The arrival times of these phases at

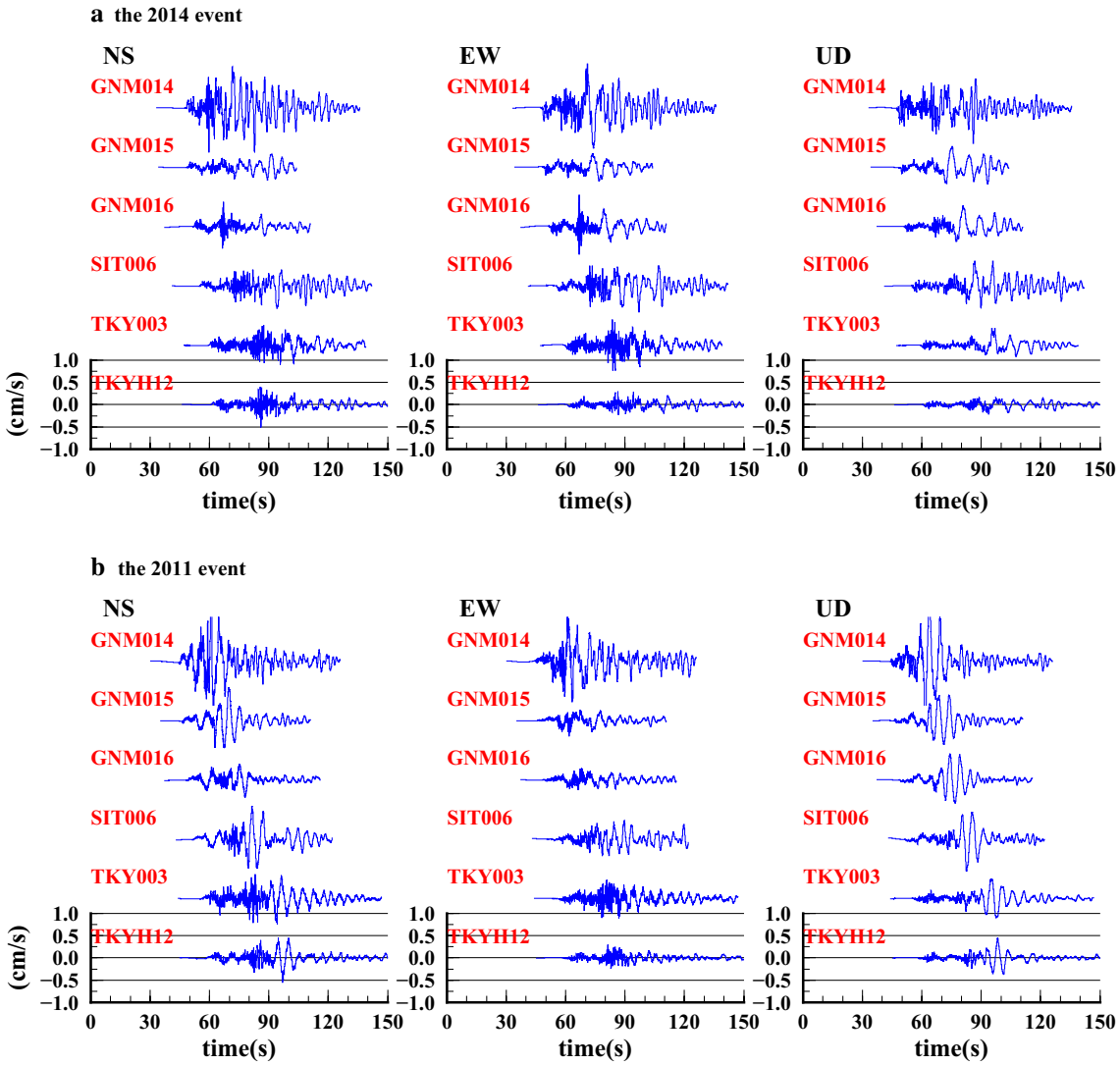

Fig. 6 Velocity waveforms at the stations located in the outside the basin area. **b** Show the 2011 event waveforms; **a** show those of the 2014 event. *Columns from left to right* show the NS, EW, and UD components, respectively. *Characters associated with each trace* indicate the station code. The location of each station is shown in Fig. 2

the stations on the east shore of Tokyo Bay are later than those at the stations on the west shore, and there are no significant phases at the YKS, MYK, and FUT stations. There are no significant wave packets in the waveforms of the 2014 event, but the dominant period of the S-wave part in the horizontal components is longer than that of the 2011 event. In the waveforms of the NS component at GOI and CHB stations, the later arrivals with predominant periods of 6–8 s are recognized at around 200 s for both events. However, the predominant period of these wave packets and arrival time difference between GOI and CHB vary between the two events.

The velocity response spectra with 5% damping are compared in Fig. 4. The response spectra of the 2011 event have remarkable peaks at around 5 s in the horizontal and vertical components at all stations except for YKS. In the response spectra from CHB, the peak period in the NS component is longer than the peak period for other stations. The response spectra of the 2014 event have no significant 5-s peaks, and the peak period is longer than that of the 2011 event. There are significant peaks with periods of 7–8 s in the SNG spectrum for only the horizontal component and in the CHB spectrum for all components.

The arrival times of the significant later phases at the stations located on the west side are faster than those stations located on the east side of Tokyo Bay, as shown in Fig. 3. This suggests that these later phases propagated from west to east. To confirm this hypothesis, we provide the velocity waveforms at stations on west–east direction observation line north of Tokyo Bay in Fig. 5. The top two traces are velocity seismograms at the station located outside of the basin, and the other eight traces are velocity seismograms at the station in Kanto Basin. These traces show that the long-period wave packets propagated from west to east in the basin area.

Ground motions at the stations located outside of the basin

The ground motions outside the Kanto Basin were studied to examine the properties of the incident wave. The velocity waveforms at stations outside the basin are shown in Fig. 6. The station locations are shown in Fig. 2 with blue circles. A remarkable later phase is confirmed in the NS and UD components of the 2011 event. This phase seems to propagate from north to south. In contrast, no special later arrival was recognized in the velocity seismograms from the 2014 event.

The velocity response spectra with 5% damping are shown in Fig. 7. A significant peak, with a 5-s period, is apparent in the velocity response spectra of the 2011 event. This peak is coincident with the predominant period of the significant later phases in the basin area. However, this significant later phase was not recognized in the waveforms of the 2014 event, and there is no significant peak in the 2014 event spectra. The difference between the 2011 and 2014 incident waves to the basin caused the variation in the observed ground motions in the Tokyo Bay area.

To evaluate the wave type of the later phase, particle motions were produced using the velocity waveforms at station TKY003 for the 2011 event, as shown in Fig. 8. The NS and the EW components were converted to the radial and transverse components using the back azimuth to the epicenter. The significant later phase is in the time window between 45 and 60 s. The vibrations of the later phase are dominantly in the radial direction, and orbital motion in the radial UD plane shows retrograde rotation to the radial direction. From this evidence, the significant later phase is interpreted as Rayleigh waves.

Discussion

Effects of source region velocity structure

The Rayleigh waves observed at the stations located outside the basin were likely excited in the source region. The contouring of the seismic bedrock depth shown in Fig. 2 suggests that the velocity structures in the two source regions are different. The structure of the outside the basin area surrounding Kanto Basin is also different from the structures of the source regions. We studied

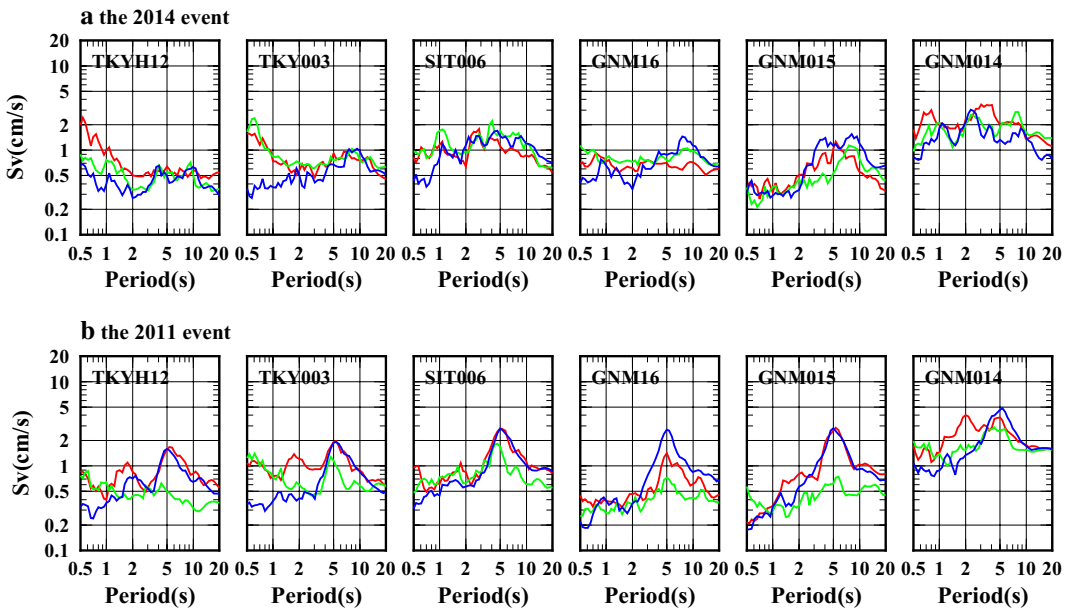

Fig. 7 Velocity response spectra at stations located in the outside the basin area. **b** Show the 2011 event spectra; **a** show those of the 2014 event. *Red*, *green*, and *blue lines* indicate the spectra of the NS, EW, and UD components, respectively. *Characters in each frame* indicate the station code. The location of each station is shown in Fig. 2

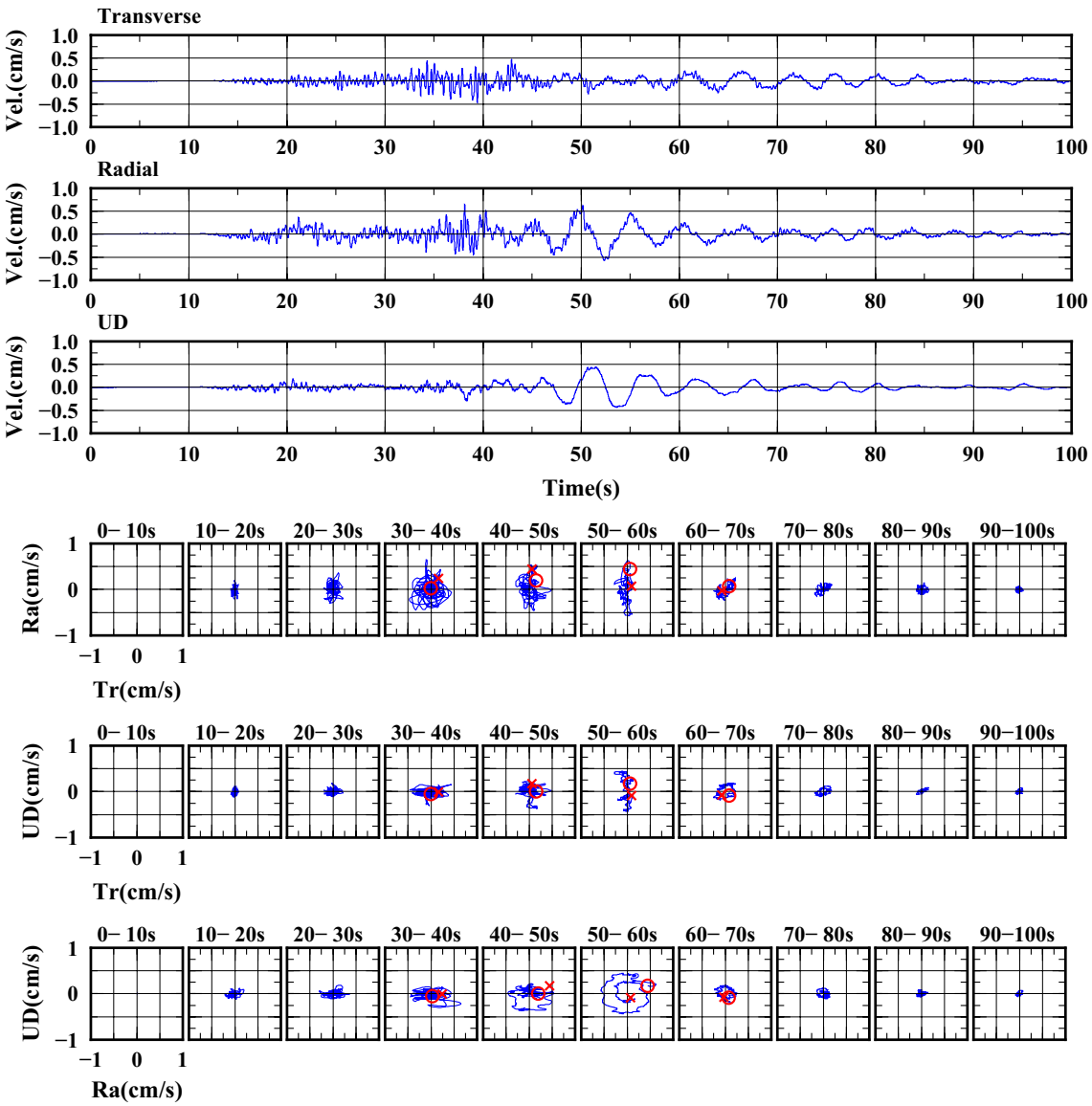

Fig. 8 Particle motion from velocity seismograms at station TKY003 during the 2011 event. The *three bottom rows* indicate the particle motions in the radial *vertical* (UD) plane, transverse *vertical* (UD) plane, and transverse radial *horizontal plane*. The particle motions are displayed every 10 s. *Red circles* and *crosses* indicate the start and end points, respectively. The *three top figures* are velocity traces in the transverse, radial, and UD components, respectively

the Rayleigh wave propagation characteristics using 2-D velocity structure models as shown in Fig. 9. These models were made by connecting the source region with the outside the basin area based on the "Japan Integrated Velocity Structure Model version 1" (Koketsu et al. 2012). The seismic bedrock (layer no. 8) is deep in the source region but very shallow in the outside the basin area.

A fourth-order staggered grid FDM was used for the P-SV problem. The model size was 60 km in the horizontal direction and 30 km in the depth direction with a 50-m grid size. The bottom, left, and right sides of the model were set with absorbing boundary conditions (Cerjan et al. 1985). The Q value was taken into account according to Graves (1996), and the reference frequency was 0.2 Hz. The time step of calculation was 0.002 s. We set the same moment source based on a reverse fault with a dip of 45° at 6 km depth in both simulations. The Herrmann function (Herrmann 1979) with a 5-s period was used as the source function.

The results from the two models are compared in Fig. 10. The later arrivals in the traces of the 2011 event model are more pronounced than those in the traces of

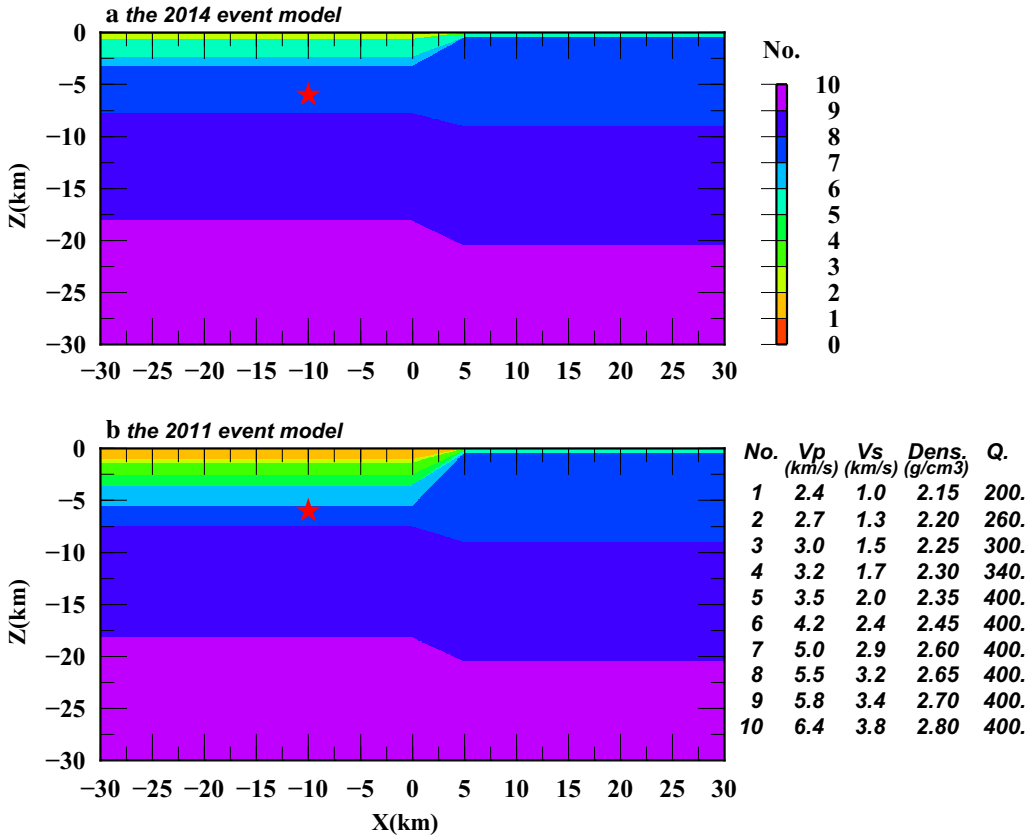

Fig. 9 2-D velocity structure models using a comparison of wave propagation characteristics. *Lower* and *upper* models correspond to the source regions for the 2014 and 2011 events, respectively. *Red stars* indicate the source points. *Color contours* show the layer numbers. The table at the *lower right* provides the layer properties

the 2014 event model, especially in the deep bedrock area ($X < 0.0$). In the shallow bedrock area ($X > 5.0$), the later arrivals of the 2011 event model are also delayed and larger than those of the 2014 event model. However, the difference in amplitude between the two models is not as large as in the observation records. We hypothesize that the differences between the observations and model results are due to the simplified simulation; the actual ground motions contain the combined effects of 3-D subsurface structures and detailed fault ruptures. Zama (1996) made the pioneering proposal to consider the combination of focal region and target region at the time long-period ground motion is evaluated. When evaluating earthquake ground motion, we should consider not only the seismic parameters but also the velocity structure of the focal region.

Effects of basin features on surface wave propagation

The deep bedrock area of the Kanto Basin extends in the northwest direction similar to a trench, as shown in Fig. 2, and this structure guides the propagation of surface waves. Koyama et al. (1988) reported that this trench guided the propagation of Love waves from events that occurred in western Nagano Prefecture. Furumura and Hayakawa (2007) reported that long-period ground motions observed in the Tokyo area during the 2004 Niigata-ken Chuetsu M6.8 earthquake were propagated thorough this trench. The epicenter of this earthquake was located about 40 km north of the epicenter of the 2011 event. Therefore, the effect of this trench on the later arrivals during the 2011 event was studied from a consideration of travel time. The velocity waveforms in the NS and UD components are shown in Fig. 11. The first onset of S waves propagated from north to south with almost the same velocity outside the basin area as in the trench-like basin area. However, long-period later arrivals in the trench-like basin area propagated more slowly than those in the outside the basin area. The significant later arrivals in the trench-like basin area and significant later arrivals in the Tokyo Bay area were not temporally continuous. The significant later arrivals in the Tokyo Bay area likely propagated from

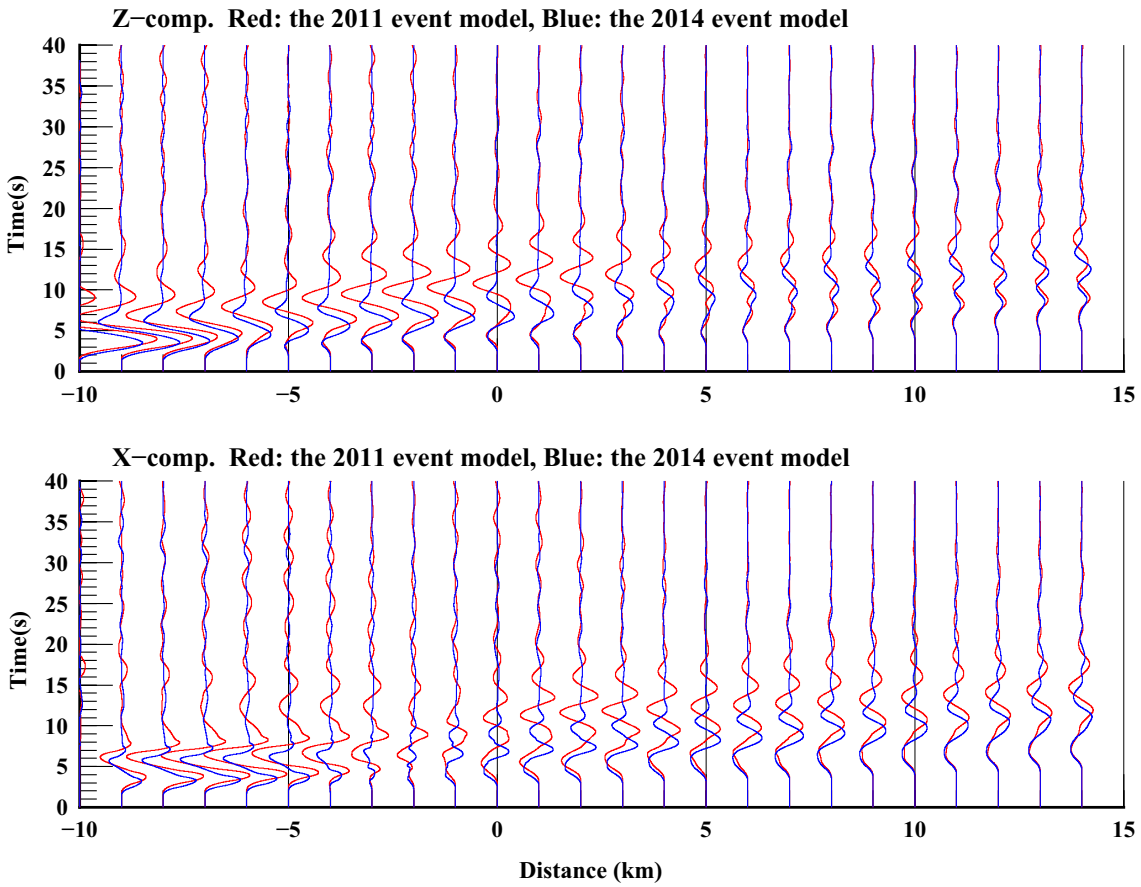

Fig. 10 Comparison of ground motion traces using different velocity structures in the source regions. *Red* and *blue lines*, respectively, show the ground motion traces using the 2014 and 2011 event models shown in Fig. 9

around TKYH12, as shown in Fig. 5. The later arrivals with a predominant period of 5 s were likely excited by the incidence of Rayleigh waves from outside the basin area to the basin. The excitation and propagation of significant later arrivals with a predominant period of 5 s during the 2011 event were not affected by the trench-like structure of the Kanto Basin.

Yuzawa and Nagumo (2012) studied the shakability of long-period ground motion in Kanto Basin and pointed out that its variability is due to source region. They interpreted the amplitude variation as due to the distance that the surface wave travels through sedimentary layers. Our results indicate that the variation in shakability is not only affected by propagation distance in the basin but also by input wave characteristics.

Conclusions

A shallow M6.7 earthquake occurred in northern Nagano Prefecture, Japan, on November 22, 2014. The magnitude, focal depth, and source mechanism of this event were almost identical to an event that occurred near the border of Nagano and Niigata prefectures on March 12, 2011. However, the seismograms of these events observed from the Tokyo Bay area were quite different. Significant long-period later arrivals with a predominant period of 5 s were recognized in the traces of the 2011 event, but were not recognized in the traces of the 2014 event. Because the incident wave to the Kanto Basin is a controlling factor on long-period ground motion in the Tokyo Bay area, we examined the ground motion at an outside the basin site. A large wave packet with a predominant period of 5 s was clearly recognized in the velocity traces of the 2011 event. This wave packet was likely a Rayleigh wave. From a numerical simulation, we confirmed that the subsurface structure of the focal region affected the excitation of the Rayleigh waves. Therefore, the difference in long-period ground motion between the two events in the Tokyo Bay area was affected by excitation of Rayleigh waves in the focal regions. This suggests that it is important to consider the effects of both the local and source regions.

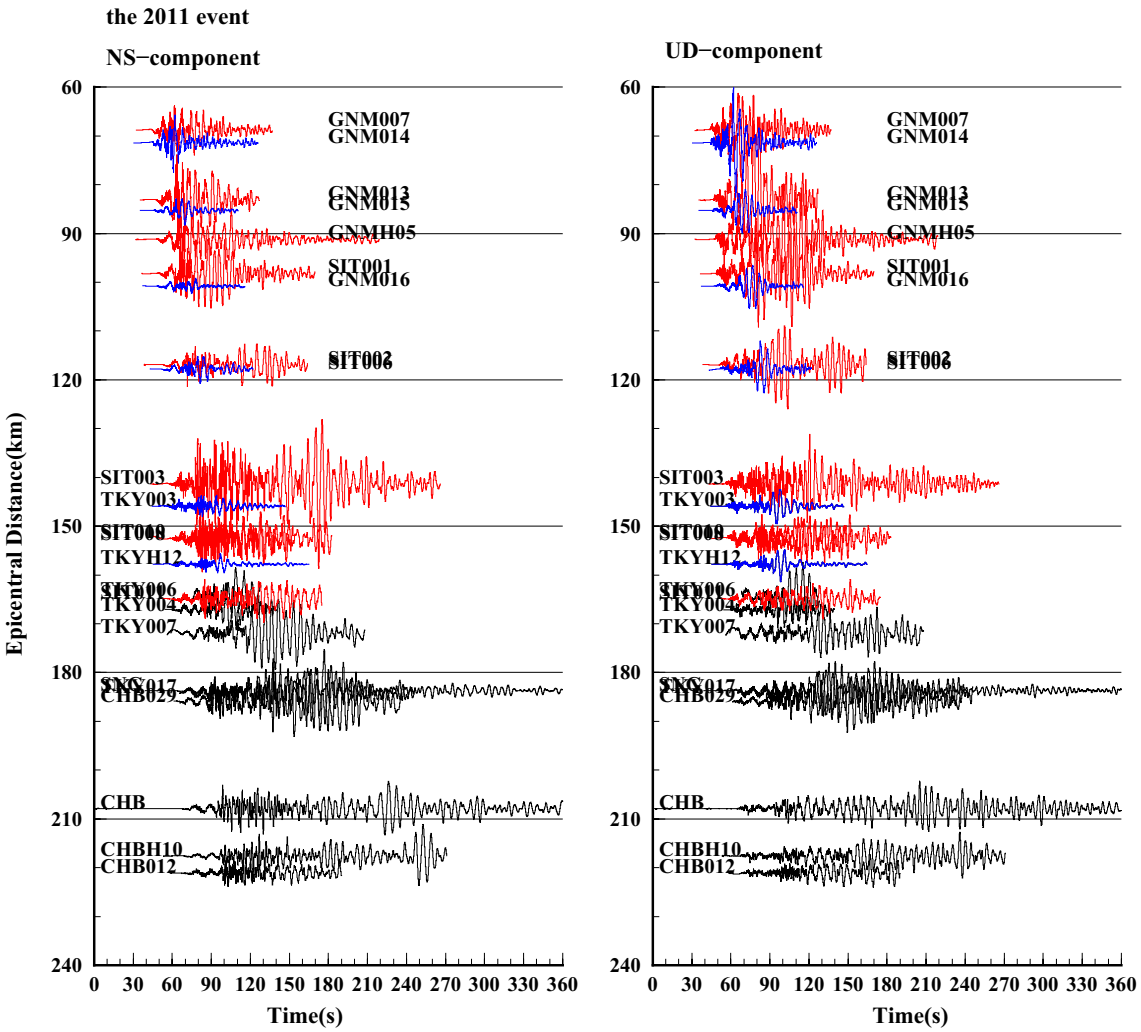

Fig. 11 Sections of velocity seismograms observed during the 2011 event. The *left-side figure* shows the traces in the NS component. The *right-side figure* shows the traces in the UD component. *Red traces* are observed at stations on the deep trench of the Kanto Basin, as shown in Fig. 2. *Blue traces* indicate the ground motions at stations located outside the basin, as shown in Fig. 2. *Black traces* indicate the stations used in Fig. 5

Acknowledgements
The source parameters for the earthquakes used in this study were provided by the Japan Meteorological Agency. The CMT solution for the F-net and strong motion data from K-NET and KiK-net were provided by the National Research Institute for Earth Science and Disaster Resilience, Japan. Generic Mapping Tools (Wessel and Smith 1998) was used to draw the figures. Editor Takuto Maeda, reviewer Yadab P. Dhakal, and an anonymous reviewer helped to significantly improve the manuscript.

Competing interests
The author declares that he/she has no competing interests.

Publisher's Note

Received: 21 December 2016 Accepted: 16 May 2017
Published online: 22 May 2017

References

Cerjan C, Kosloff D, Kosloff R, Reshelf M (1985) A nonreflecting boundary condition for discrete acoustic and elastic wave equations. Geophysics 50:705–708

Fukuyama E, Ishida M, Dreger DS, Kawai H (1998) Automated seismic moment tensor determination by using on-line broadband seismic waveforms. J Seismol Soc Jpn (Zisin 2) 51:149–156 **(in Japanese with English abstract)**

Furumura T, Hayakawa T (2007) Anomalous propagation of long-period ground motions recorded in Tokyo during the 23 October 2004 Niigata-ken Chuetsu (Mw6.6) earthquake, Japan. Bull Seismol Soc Am 97(3):863–880

Graves RW (1996) Simulating seismic wave propagation in 3D elastic media using staggered-grid finite differences. Bull Seismol Soc Am 86:1091–1106

Herrmann RB (1979) SH-wave generation by dislocation source—a numerical study. Bull Seismol Soc Am 69:1–15

Japan Meteorological Agency (JMA) (2016) The Seismological Bulletin of Japan. http://www.data.jma.go.jp/svd/eqev/data/bulletin/hypo_e.html. Accessed 18 Dec 2016

Kanno T, Narita A, Morikawa N, Fujiwara H, Fukushima Y (2006) A new attenuation relation for strong ground motion in Japan based on recorded data. Bull Seismol Soc Am 96(3):879–897. doi:10.1785/0120050138

Koketsu K, Miyake H, Suzuki H (2012) Japan integrated velocity structure model version 1. In: Proceedings of the 15th world conference on earthquake engineering. Paper no. 1773

Koyama S, Seo K, Samano T (1988) On the significant later phase of seismograms at Kumagaya, Japan. In: Proceedings of 9th world conference on earthquake engineering, vol 2, pp 585–590

Okada Y, Kasahara K, Hori S, Obara K, Sekiguchi S, Fujiwara H, Yamamoto A (2004) Recent progress of seismic observation networks in Japan—hi-net, K-NET and KiK-net. Earth Planets Space 56:xv–xxviii. doi:10.1186/BF03353076

Wessel P, Smith W (1998) New, improved version of the generic mapping tools released. EOS Trans AGU 79:579

Yokota T, Ikeuchi K, Yahagi T, Kaida Y, Suzuki H (2011) Attenuation and amplification of long-period component of ground motion. J Jpn Assoc Earthq Eng 11(1):1_81–1_101. doi:10.5610/jaee.11.1_81 **(in Japanese with English abstract)**

Yuzawa Y, Nagumo H (2012) Factors of variability and measures for the shakability of long-period ground motion—Kanto Basin as an example. J Jpn Assoc Earthq Eng 12(2):2_41–2_59 **(in Japanese with English abstract)**

Zama S (1996) Regionality of long-period ground motion using JMA strong motion displacement records. In: Proceedings of 11th world conference on earthquake engineering. Paper 1891